Elsevier Editorial System(tm) for Annals of Anatomy
Manuscript Draft

Manuscript Number:

Title: ULTRASTRUCTURAL STUDY OF CULTURED OVINE BONE MARROW-DERIVED MESENCHYMAL STROMAL CELLS

Article Type: Research Article

Keywords: ovine, bone marrow, MSCs, flow cytometry, transmission electron microscopy

Corresponding Author: Prof. Salvatore Desantis,

Corresponding Author's Institution: University of Bari

First Author: Salvatore Desantis

Order of Authors: Salvatore Desantis; Gianluca Accogli; Sara Zizza; Maria Mastrodonato; Antonella Blasi; Edda Francioso; Roberta Rossi; Antonio Crovace; Leonardo Resta

Abstract: Ovine bone marrow-derived mesenchymal stromal cells (oBM-MSCs) represent a good animal model for cell-based therapy and tissue engineering. Despite their use as a new therapeutic tool for several clinical applications, the morphological features of oBM-MSCs are yet unknown. Therefore, in this study the ultrastructural phenotype of these cells was analysed by transmission electron microscopy (TEM). The oBM-MSCs were isolated from the iliac crest, cultured until they reached near-confluence. After trypsinization, they were processed to investigate their ultrastructural features as well as specific surface marker proteins by flow cytometry and immunogold electron microscopy. Flow cytometry displayed that all oBM-MSCs lacked expression of CD31, CD34, CD45, HLA-DR whereas expressed CD44, CD58, HLAI and a minor subset of cell population exhibited CD90. TEM revealed the presence of two morphologically distinct cell types: cuboidal electron-lucent cells and spindle-shaped electron-dense cells, both expressing CD90 antigen. Most of the electron-lucent cells showed glycogen aggregates, dilated cisternae of RER, moderately developed Golgi complex, and secretory activity. The electron-dense cell type was constituted by two different cell-populations: type A cells with numerous endosomes, dense bodies, rod-shaped mitochondria and filopodia; type B cells with elongated mitochondria, thin pseudopodia and cytoplasmic connectivity with electron-lucent cells. These morphological findings could provide a useful support to identify "in situ" the cellular components involved in the cell-therapy when cultured oBM-MSCs are injected.

ULTRASTRUCTURAL STUDY OF CULTURED OVINE BONE MARROW-DERIVED MESENCHYMAL STROMAL CELLS

Salvatore Desantis[a*], Gianluca Accogli[a], Sara Zizza[a], Maria Mastrodonato[b], Antonella Blasi[c], Edda Francioso[a], Roberta Rossi[a], Antonio Crovace[a], Leonardo Resta[a]

[a]Department of Emergency and Organ transplantation; University of Bari "Aldo Moro", Italy
[b]Department of Biology - University of Bari "Aldo Moro", Italy
[c]Medestea Research and Production Laboratories, Consorzio CARSO, Bari, Italy

*Corresponding author: Salvatore Desantis, Department of Emergency and Organ Transplantations, University of Bari Aldo Moro, S.P. Casamassima Km. 3, 70010 Valenzano, Italy.

Tel.:+39-080-544-3801; fax: +39-080-544-3801

E-mail: salvatore.desantis@uniba.it

Summary

Ovine bone marrow-derived mesenchymal stromal cells (oBM-MSCs) represent a good animal model for cell-based therapy and tissue engineering. Despite their use as a new therapeutic tool for several clinical applications, the morphological features of oBM-MSCs are yet unknown. Therefore, in this study the ultrastructural phenotype of these cells was analysed by transmission electron microscopy (TEM). The oBM-MSCs were isolated from the iliac crest, cultured until they reached near-confluence. After trypsinization, they were processed to investigate their ultrastructural features as well as specific surface marker proteins by flow cytometry and immunogold electron microscopy. Flow cytometry displayed that all oBM-MSCs lacked expression of CD31, CD34, CD45, HLA-DR whereas expressed CD44, CD58, HLAI and a minor subset of cell population exhibited CD90. TEM revealed the presence of two morphologically distinct cell types: cuboidal electron-lucent cells and spindle-shaped electron-dense cells, both expressing CD90 antigen. Most of the electron-lucent cells showed glycogen aggregates, dilated cisternae of RER, moderately developed Golgi complex, and secretory activity. The electron-dense cell type was constituted by two different cell-populations: type A cells with numerous endosomes, dense bodies, rod-shaped mitochondria and filopodia; type B cells with elongated mitochondria, thin pseudopodia and cytoplasmic connectivity with electron-lucent cells. These morphological findings could provide a useful support to identify “in situ” the cellular components involved in the cell-therapy when cultured oBM-MSCs are injected.

Key words: ovine, bone marrow, MSCs, flow cytometry, transmission electron microscopy

1. Introduction

The mesenchymal stromal cells (MSCs), first described by Friedenstein et al. (1970) as population of bone marrow stromal cells that were able to adhere to the plastic culture substrate, aremultipotent cells present in bone marrow which can replicate as undifferentiated cells and have differentiation potential giving rise to mesenchymal tissue lineages such as bone, cartilage, fat, tendon, muscle, and marrow stroma (Prockop, 1997; Pittenger et al., 1999). These cells can also become neurons, cardiac muscle cells and corneal keratocytes under specific conditions (Makino et al., 1999; Holden and Vogel, 2002; Jiang et al., 2002; Dezawa et al., 2004; Takayama et al., 2009).

In human , MSCs are defined by several key features: they strongly adhere to a plastic surface in culture; they are clonogenic; they show a surprising proliferation rate (self-renewing); they exhibit a remarkable plasticity, being able to differentiate into many mature cell types of mesodermal and non mesodermal origin (multipotency) (Bruder et al., 1997; Pittenger et al., 1999; Woodbury et al., 2000; Payushina et al., 2006). In addition to these features, the Mesenchymal and Tissue Stem Cell Committee of the International Society for Cellular Therapy (ISCT) considers the MSCs as plastic-adherent cells which express the surface markers CD73, CD90 and CD105 and lack expression of CD14 or CD11b, CD34, CD45, CD79 or CD19 and HLA-DR (Dominici et al., 2006). Besides the markers defined by the ISCT, additional surface proteins have been reported to be expressed by human MSCs including CD29, CD44, CD106 and CD166 (Pittenger et al., 1999; Barry and Murphy, 2004).

In contrast to human MSCs, no uniform characterization criteria are available to date for animal origin MSCs in general, including ovine MSCs. For example, in ovine bone marrow derived MSCs (oBM-MSCs) the expression of CD90 has been detected by Rentsch et al.(2010) but not byMcCarty et al.(2009) and Rozemuller et al. (2010).

Due to their low immunogenicity and lack of alloreactivity MSCs are considered as optimal candidates for transplantation procedures (Bartholomew et al., 2002; Gotherstrom, 2007; Nauta and Fibbe, 2007; Mobasheri et al., 2009). Recently, numerous experimental studies have demonstrated that oBM-MSCs are good animal model for cell-based therapy and tissue engineering. oBM-MSCs are able to promote bone formation in induced osteonecrosis (Feitosa et al., 2010), tibial defect (Field et al., 2011) and in a ceramic bone substitute (Boos et al., 2011). Additionally, these cells permit the regeneration of injured growth plate cartilage (McCarty et al., 2010) and articular chondrocytes (Marquass et al., 2011). Lastly, oBM-MSCs are effective in regeneration of tendon tissue after induced tendinitis (Crovace et al., 2008; Lacitignola et al, 2014).

In spite of their considerable importance in the cell-based therapy, detailed ultrastructural studies of the adult MSCs are scarce in mammals (Seed et al., 1986; Pasquinelli et al., 2007; Karaöz et al., 2011) and lack in ovine. The objective of this study was to examine the ultrastructural features of the oBM-MSCs. Since in the tissues of adult mammals a diffuse network of MSCs exists, the knowledge of their ultrastructural characteristics could represent the basis to identify "in situ" the niches in which such cells reside. Consequently this could provide a functional support for maturation of precursors of the primary cellular compartments in adult tissues as it has beensuggested for humans (Pasquinelli et al., 2007).

2. Materials and methods

2.1. Bone marrow harvesting

This study was part of a larger research that included the harvest of ovine bone marrow. The ethical committee of the University of Bari in accordance with National animal welfare legislation, and in compliance with the guidelines outlined in the NRC Guide for the Care and Use of Laboratory Animals, approved the use of ewes (Bergamasca breed, 2 years of age, female, 45 kg in weight, not inbred) for the study.

Bone Marrow (BM) samples were obtained from the iliac crest of 2 healthy sheeps according to Crovace et al. (2008). The procedure was performed under sedation with diazepam[a] (0.05 mg/kg) and local anaesthesia with lidocaine chlorhydrate[b] 2% (20 ml) around the tuber coxae. After aseptic preparation of skin, a 14 gauge (1.0 mm) jamshidi needle was inserted in the tuber coxae to a depth of 3–4 cm. A 20 ml heparinazed (2500 I.U. heparin/20 ml BM) syringe was attached to the needle to obtain BM.

2.2. Cell Culture

The BM were diluted 1:1 in PBS, then stratified 1:1 on Biocoll Separating solution (FICOLL, gradient 1,077 g/ml, Biochrom, Berlin,Germany) and centrifuged at 2000 rpm x30 min and were seeded in flasks at a concentration of 4–5 x 10^6 cells/cm^2 in complete medium (Coon's) at 37°C in a humid 5% CO2/air (carbogen) atmosphere. Non-adherent cells were discarded after 3 days and adherent cells were cultured until they reached near-confluence (10 days) (Fig. 1). The cultures of BMSCs were trypsin-treated in a routine manner and, after collection in Falcon tubes, the detached cells were rinsed in PBS and centrifuged twice at 1200 rpm for 10 min.

2.3. Flow cytometric analysis

Flow cytometric analysis was used to characterize the cell-surface antigen expression of oBM-MSCs using antibodies against positively (CD44, CD58, CD90 and HLAI) and negatively (CD31,CD34, CD45 and HLA-DR) markers associated with MSC populations. After trypsinization, cells were resuspended with FACS buffer (pH 7.2 PBS, BSA 0.5%, sodium azide 0.02%) at a concentration of 0.1 x 10^6/100 µl and were labelled for 30 min at room temperature in the dark using 10 µl (1:10 dilution) of fluorochrome-unconjugated mouse primary antibodies anti-ovine CD44 (Serotec®, Milan, Italy) and anti-human CD90 (BD Biosciences Pharmingen, San Diego,CA) or fluorochrome-conjugated monoclonal anti-ovine antibodies anti-CD45FITC,anti- HLA I FITC, anti-CD31PE, anti-CD34PE, anti-CD58PE, and anti- HLA-DR PE (Serotec®, Milan, Italy). Then the cells were washed with FACS buffer to remove non-conjugated antibodies and those incubated with anti CD44 and CD90 were incubated with fluorescein isothiocyanate (FITC)-Goat anti-mouse IgG (H+L) secondary antibody (R&D®, dilution 1:10) for 30 minutes at room temperature in a dark room. Epics `XL-MCL' (Beckman Coulter) flow cytometer was used to analyse fluorescent phenotypic marker signals. At least 10,000 events for test sample were acquired. The negative control assay was performed by the reaction of each primary antibody with the respective peptide antigen. Sample histogram elaboration was performed with EXPO 32 software toassess fluorescent distribution (Fig. 2).

2.4. Electron microscopy

The pellets were fixed with 2.5% glutaraldehyde in 0.1 M phosphate buffer (TBS), pH 7.3, for 2 h at room temperature, and post-fixed or not with 1% OsO_4 in the same buffer for 1 h. Samples were dehydrated in an ethanol series and embedded in Epon 812.

Semithin sections (1 µm thick) were cut and stained with saturated, borax-buffered toluidine blue dye solution and examined under light microscopy to study the general morphology.

Ultrathin sections (50-70 nm) with silver interference were cut, picked up on copper grids and stained with uranyl acetate and lead citrate.

2.5. Immunoelectron microscopy

Ultra-thin sections were mounted on formwar-coated gold grids and incubated overnight with the mouse antibody against human CD 90 (BD Biosciences Pharmingen, San Diego, CA) diluted 1:50 in blocking buffer (TBS 0.1M, pH 7.4 + BSA1%) at 4 °C. Grids were rinsed with TBS (0.1M, pH 7.4), and then incubated at a dilution of 1:20 of 10-nm gold-conjugated anti mouse IgG (Sigma) in TBS for 1 h at RT. After several rinses in TBS, the grids were lightly stained with uranyl acetate and lead citrate. Negative controls were performed by substituting the primary antibody with TBS.

The grids were observed under a Morgagni 268 electron microscope (FEI, Hillsboro, Oregon, USA).

3. Results

3.1. Expression of cell surface markers

Cultured MSC represented a heterogeneous population of cells. We found that oBM-MSCs were uniformly positive for CD44, CD58, and HLA I expression, whereas a minor population of cells exhibited CD90. oBM-MSCs lacked expression of the endothelial marker (CD31), hematopoietic markers (CD34 and CD45), and immunological marker (HLA-DR) (Fig. 2)., thus confirming a MSC immunophenotype.

3.2. Light microscopy

Semithin sections stained with toluidine blue showed that sBM-MSCs contained two distinct kinds of cells: weakly stained large cuboidal cells and strongly stained spindle-shaped cells (Fig. 3).

3.3. Transmission electron microscopy

TEM observations revealed the presence of two cell types: electron-lucent cells and electron- dense cells. sBM-MSCs exhibited large, irregularly and euchromatic nuclei with one or two nucleoli.

The electron-lucent cells were cuboid in shape and in the cytoplasm were distributed intermediate filaments, elongated mitochondria with dense matrix, glycogen that sometime constitutes large aggregates in the peripheral zone (Figs. 4A,B). Scattered in the cytoplasm it was the rough endoplasmic reticulum (RER) with prominent dilated cisternae containing moderately electron-dense material (Figs. 4A,B). Golgi complex was moderately developed (Fig. 4C). Inaddition, the release of moderately electron-dense material from secretory vesicles (Fig. 4D) as wellas receptor-mediate endocytosis were observed (Fig. 4E). Lastly, cell junctions with other light cellsand with dark cells were present (Figs. 4B,F).

Some electron-lucent cells appeared to be characterized by endocytic vesicles, primary and secondary lysosomes, residual bodies and vacuoles giving the cytoplasm a multivacuolated appearance (Figs. 5A,B). Moreover, the presence of elongated mitochondria with electron-dense matrix were another common feature (Fig. 5B).

Two sub-populations of electron-dense cells were distinguished: type A and type B cells (Figs. 6A,D). Type A dark cells were sferoid in shape, and showed numerous filopodia on their surface (Fig. 6A). Their cytoplasm displayed glycogen aggregates, large vesicles containing different type

of matrix (Fig. 6A), RER profiles, scarce lipid droplets, endocytic vesicles (Fig. 6B), as well as rod-shaped mitochondria with pale matrix (Fig. 6C). Type B electron-dense cells were spindle-shaped cells with high content of glycogen which constituted large aggregates (Fig. 6E). RER profiles were moderately scattered in the cytoplasm which showed elongated mitochondria with dense matrix (Fig. 6E). The nucleus, irregular in shape, contained finely dispersed heterochromatin. The cell surface showed thin pseudopodia (Fig. 6D) as well as intercellular junctions and cytoplasmicconnections with electron-lucent cells (Figs. 6E,F).

The immunogold electron microscopy revealed that surface CD90 antigen is expressed in both electron-lucent cells and electron-dense cells (Figs. 7A,B).

4. Discussion

Bone marrow contains at least two kinds of stromal cells, hematopoietic stem cells and stem cells for nonhematopoietic tissues (Friedenstein et al.,1970), referred as mesenchymal stem cells or marrow stromal cells (MSCs). The ability of MSCs to differentiate into many mature cell types of mesodermal and nonmesodermal origin allows their use in the mammal regenerative medicine, including sheep.

There is very little information available on the cell surface characteristics of oBM-MSCs, because of the paucity of antibodies specific for sheep. However, in this study the used anti-ovine antibodies against CD31, CD34, CD45, HLA-DR did not positively react with oBM-MSC. This is consistent with the absence of expression in human MSCs of the endothelial and haematopoietic markers (CD34, CD45, HLA-DR) (Dominici et al., 2006). The absence of leukocyte antigen HLA- DR expression confirmed the immunosuppressive potential of ovine. In addition, these cultured cells strongly expressed surface antigens such as CD44, CD58 and HLAI which are typically expressed in MSCs (De Girolamo et al., 2013. Furthermore, our cell cultures contained a minor population of cells (12%) expressing CD90, a further positive MSC marker (Wiesmann et al., 2006)which in ovine MSCs was previously displayed only by Rentsch et al. (2010) (although the percentage of positive cells was not reported) but not by other researchers (McCarty et al.,2009; Rozemuller et al.,2010; Kalaszczynska et al., 2013). This result could depend on the cross-reactivityof the antibodies used

The present study for the first time demonstrates the ultrastructural features of cultured oBM-MSCs, which are considered profitably models for cell-based therapy in sheep (Crovace et al., 2008; Feitosa et al., 2010; McCarty et al., 2010; Boos et al.,2011; Field et al., 2011; Marquass et al. 2011; Lacitignola et al., 2014).

Cultures of oBM-MSCs consisted of large cuboidal electron-lucent cells and spindle-shaped (flattened) electron-dense cells. The immunoelectron microscopy revealed that both the cell types expressed the CD90 surface antigen. In accordance with the flow cytometric analysis, this result demonstrates that our investigated cells are MSCs. Indeed, CD90 is commonly used as a positive surface marker for MSC (Ghilzon et al., 1999; Dominici et al., 2006; Wiesmann et al., 2006). Previous studies demonstrated that human BM-MSCs contain at least two morphologically distinct kinds of cells (Colter et al., 2001).

Most of the electron-lucent cells showed the ultrastructural features described in the literature for the MSCs, such as the presence of glycogen aggregates, dilated cisternae of RER, moderately developed Golgi complex (Baharvand and Matthaei, 2003; Pasquinelli et al., 2007; Karaöz et al., 2011). In addition, in this study the presence of a secretory activity was observed. This suggests that oBM-MSCs contain the glycoprotein synthesis machinery and that the secretion of glycoproteins may occur. These macromolecules are crucial for the development, growth, functioning of the cells because they have structural, modulatory and recognition properties (Varki and Lowe, 2009). MSCs have great therapeutic potential because of their secretion of a great variety of cytokines and growth factors that mediate anti-apoptotic, angiogenic, immunoregulatory and anti-scarring processes, along with others (Meirelles and Nardi., 2009; Somoza et al., 2015).

Some of electron-lucent cells showed multivacuolated cytoplasm due to the presence of endocytic vesicles and lysosomes, which suggest that these cells are involved in the endocytotic anddigestive activity of molecules from the culture medium. On the basis of these ultrastructuralfeature it is possible to infer that these two sub-population of electron-lucent cells could represent different stages of activity of the same cell type. The presence of clear blisters, vacuoles and vesicles, evocative of intense endocytic activity have been described in hBM-MSCs (Colter et al., 2001; Pasquinelli et al., 2007; Karaöz et al., 2011).

The electron-dense oBM-MSCs population was constituted by cells containing glycogen aggregate, RER profiles and filopodia. However, this oBM-MSCs population seems to be constituted by two different cell-types: type-A cells and type-B cells. The prominent feature of typeA cells was the presence of numerous endosomes, dense bodies and filopodia not implicated in cell- to-cell interations. This suggests that they are involved in endocytotic activity and are migrating cells.

Type B cells displayed some large vacuoles, but their main characteristic was the presence of thin pseudopodia some of them involved in the intercellular junction with electron-lucent cells. In addition, points of contact with light cells were established where cytoplasmic connectivity was seen. This suggests that oBM-MSCs can also communicate by a direct intercellular cytoplasmic

molecule transfer. This type of cell-to-cell communication need ATP consumption because long mitochondria were seen in their proximity. Recent reports have shown that intercellular transfer of organelles as well as membrane components and cytoplasmic molecules can be mediated by cellular extensions (Gurke et al., 2008; Hurtig et al., 2010). However, conventional intercellular junctions have been observed in the hBM-MSCs by Karaöz et al. (2011).

The above described ultrastructural features suggest that oBM-MSCs contain different cell sub-populations. This is also supported by the morphology of mitochondria that were elongated with dense matrix in electron-lucent cells and type-B dark cells , whereas they were rod-shaped in type- A dark cells. It is well known that mitochondria morphology can differ among cell-types. It has been recently reported that at least two morphologically distinct forms of BM derived cells are distributed in the mouse cornea using BM transplantation. Most of BM-derived cells have a macrophage lineage, while some cells in the corneal stroma do not (Takayama et al., 2009).

In conclusion, the present study show that oBM-MSCs contain at least two morphologically distinct kinds of cells. These ultrastructural findings could provide a morphological support to identify "in situ" the cellular components involved in the cell-therapy and tissue engineering when cultured oBM-MSCs are injected.

Acknowledgements: Authors are grateful to Dr. Luigi Balducci for its valuable suggestion during manuscript preparation.

This document was partially funded by the University of Bari "Aldo Moro", Italy.

5. References

Baharvand, H., Matthaei, K.I., 2003. The ultrastructure of mouse embryonic stem cells. Reprod. Biomed. Online 7, 330-335.

Barry, F.P., Murphy, J.M., 2004. Mesenchymal stem cells: clinical applications and biological characterization. Int. J. Biochem. Cell Biol. 36, 568–584.

Bartholomew, A., Sturgeon, C., Siatskas, M., Ferrer, K., McIntosh, K., Patil, S., Hardy, W.,Devine, S., Ucker, D., Deans, R., Moseley, A., Hoffman, R., 2002. Mesenchymal stem cells suppress lymphocyte proliferation in vitro and prolong skin graft survival in vivo. Exp. Hematol. 30**,** 42-48.

Boos, A.M., Loew, J.S., Deschler, G., Arkudas, A., Bleiziffer, O., Gulle, H., Dragu, A., Kneser, U., Horch, R.E., Beier J.P., 2011. Directly auto-transplanted mesenchymal stem cells induce bone formation in a ceramic bone substitute in an ectopic sheep model. J. Cell. Mol. Med. 15, 1364-1378.

Bruder, S.P., Jaiswal, N., Haynesworth S.E., 1997. Growth kinetics, self-renewal, and the osteogenic potential of purified human mesenchymal stem cells during extensive subcultivation andfollowing cryopreservation. J. Cell. Biochem. 64, 278-294.

Colter, D.C., Sekiya, I., Prockop D.J., 2001. Identification of a subpopulation of rapidly self-renewing and multipotential adult stem cells in colonies of human marrow stromal cells. PNAS 98, 7841-7845.

Crovace, A., Lacitignola, L., Francioso, E., Rossi G., 2008. Histology and immunohistochemistry study of ovine tendon grafted with cBMSCs and BMMNCs after collagenase-induced tendinitis. Vet. Comp. Orthop. Traumatol. 21, 329-336.

De Girolamo, L., Lucarelli, E., Alessandri, G., Avanzini, M.A., Bernardo, M.E., Biagi, E., Brini, A.T., D'Amico, G., Fagioli, F., Ferrero, I., Locatelli, F., Maccario, R., Marazzi, M., Parolini, O., Pessina, A., Torre, M.L., 2013. Mesenchymal stem/stromal cells: a new "cells as drugs" paradigm. Efficacy and critical aspects in cell therapy. Curr. Pharm. Des. 19, 2459-2473.

Dezawa, M., Kanno, H., Hoshino, M., Cho, H., Matsumoto, N., Itokazu, Y., Tajima, N., Yamada, H., Sawada, H., Ishikawa, H., Mimura, T., Kitada, M., Suzuki, Y., Ide C., 2004. Specific induction of neuronal cells from bone marrow stromal cells and application for autologous transplantation. J. Clin. Invest. 113, 1701–1710.

Dominici, M., Le Blanc, K., Mueller, I., Slaper-Cortenbach, I., Marini, F., Krause, D., Deans, R., Keating, A., Prockop, D.j., Horwitz E., 2006. Minimal criteria for defining multipotent mesenchymal stromal cells. The International Society for Cellular Therapy position statement. Cytotherapy 8, 315-317.

Feitosa, M.L., Fadel, L., Beltrão-Braga, P.C. Wenceslau, C.V., Kerkis, I., Kerkis, A., Birgel Júnior, E.H., Martins, J.F., Martins Ddos, S., Miglino, M.A., Ambrósio, C.E., 2010. Successful transplant of mesenchymal stem cells in induced osteonecrosis of the ovine femoral head: preliminary results. Acta Cir. Bras. 25, 416-422.

Field, J.R., McGee, M., Stanley, R., Ruthenbeck, G., Papadimitrakis, T., Zannettino, A., Gronthos, S., Itescu, S., 2011. The efficacy of allogeneic mesenchymal precursor cells for the repair of an ovine tibial segmental defect. Vet. Comp. Orthop. Traumatol. 2, 113-121.

Friedenstein, A.J., Chailakhjan, R.K., Lalykina, K.S., 1970. The development of fibroblast colonies in monolayer cultures of guinea-pig bone marrow and spleen cells. Cell. Tissue Kinet. 3, 393-403.

Ghilzon, R., McCulloch, C.A., Zohar, R., 1999. Stromal mesenchymal progenitor cells. Leuk. Lymphoma 32, 211-221.

Gotherstrom, C., 2007. Immunomodulation by multipotent mesenchymal stromal cells. Transplantation 84 (1 suppl.), 35-37.

Gurke, S., Barroso, J.F., Hodneland, E., Bukoreshtliev, N.V., Schlicker, O., Gerdes, H.H., 2008. Tunneling nanotube (TNT)-like structures facilitate a constitutive, actomyosin-dependent exchange of endocytic organelles between normal rat kidney cells. Exp. Cell Res. 314, 3669-3683.

Holden, C., Vogel, G., 2002. Stem cells. Plasticity: time for a reappraisal? Science 296, 2126– 2129.

Hurtig, J.,Chiu, D.T., Onfelt, B., 2010. Intercellular nanotubes: insights from imaging studies and beyond. Wiley Interdiscip. Rev. Nanomed. Nanobiotechnol. 2, 260-276.

Jiang, Y., Jahagirdar, B.N., Reinhardt, R.L., Schwartz, R.E., Keene, C.D., Ortiz-Gonzalez, X.R., Reyes, M., Lenvik, T., Lund, T., Blackstad, M., Du, J., Aldrich, S., Lisberg, A., Low, W.C., Largaespada, D.A., Verfaillie, C.M., 2002. Pluripotency of mesenchymal stem cells derived from adult marrow. Nature 418, 41–49.

Kalaszczynska, I., Ruminsk, S., Platek, A.E., Bissenik, I., Zakrzewski, P., Noszczyk, M., Lewandowska-Szumiel, M., 2013. Substantial differences between human and ovine mesenchymal stem cells in response to osteogenic media: how to explain and how to manage? Biores. Open Access 2, 356-363.

Karaöz, S., Okc, A., Gülc¸ U., Gacar, C., Sağlam, Ö., Yürüker, S., Kenar, H., 2011. A comprehensive characterization study of human Bone marrow MSCs with an emphasis on molecular and ultrastructural properties. J. Cell Physiol. 226, 1367–1382.

Lacitignola, L., Staffieri, F., Rossi, G., Francioso, E., Crovace, A., 2014. Survival of bone marrow mesenchymal stem cells labelled with red fluorescent protein in an ovine model of collagenase-induced tendinitis. Vet. Comp. Orthop. Traumatol. 27, 204-209.

Makino, S., Fukuda, K., Miyoshi, S., Konishi, F., Kodama, H., Pan, J., Sano, M., Takahashi, T., Hori, S., Abe, H., Hata, J., Umezawa, A., Ogawa, S., 1999. Cardiomyocytes can be generated from marrow stromal cells in vitro. J. Clin. Invest. 103, 697–705.

Marquass, B., Schulz, R., Hepp, P., Zscharnack, M , Aigner, T., Schmidt, S., Stein, F., Richter, R., Osterhoff, G., Aust, G., Josten, C., Bader, A., 2011. Matrix-associated implantation of predifferentiated mesenchymal stem cells versus articular chondrocytes: in vivo results of cartilage repair after 1 year. Am. J. Sports Med. 39, 1401-1412.

McCarty, R.C., Gronthos, S., Zannettino, A.C., Foster, B.K., Xian, C.J., 2009. Characterisation and developmental potential of ovine bone marrow derived mesenchymal stem cells. J. Cell Physiol. 219, 324-333.

McCarty, R.C., Xian, C.J., Gronthos, S., Zannettino, A.C., Foster, B.K., 2010. Application of autologous bone marrow derived mesenchymal stem cells to an ovine model of growth plate cartilage injury. Open Orthop. J. 23, 204-210.

Meirelles, L.S., Nardi N.B., 2009. Methodology, biology and clinical applications of mesenchymal stem cells. Front. Biosci. (Landmark Ed)14, 4281-98.

Mobasheri, A., Csaki, C., Clutterbuck, A.L., Rahmanzadeh, M., Shakibaei, M., 2009. Mesenchymal stem cells in connective tissue engineering and regenerative medicine: applications in cartilage repair and osteoarthritis therapy. Histol. Histopathol. 24, 347-366.

Nauta, A.J., Fibbe, W.E., 2007. Immunomodulatory properties of mesenchymal stromal cells. Blood 110, 3499-3506.

Pasquinelli, G.,Tazzari, P., Ricci, F., Vaselli, C., Buzzi, M., Conte, R., Orrico, C. , Foroni, L., Stella, A.,Alviano, F., Bagnara, G.P., Lucarelli, E. ,2007. Ultrastructural characteristics of human mesenchymal stromal (stem) cells derived from bone marrow and term placenta. Ultrastruct. Pathol. 31, 23-31.

Payushina, O.V., Domaratskaya, E.I., Starostin, V.I., 2006. Mesenchymal stem cells: sources, phenotype and differentiation potential. Biol. Bull. 33, 2-18.

Pittenger, M.F., Mackay, A.M., Beck, S.C., Jaiswal, R.K., Douglas, R., Mosca, J.D., Moorman, M.A., Simonetti, D.W., Craig, S., Marshak, D.R., 1999. Multilineage potential of adult human mesenchymal stem cells. Science 284, 143-147.

Prockop, D.J., 1997. Marrow stromal cells as stem cells for nonhematopoietic tissues. Science 276, 71–74.

Rentsch, C., Hess, R., Rentsch, B., Hofmann, A., Manthey, S., Scharnweber, D., Biewener, A., Zwipp, H., 2010. Ovine bone marrow mesenchymal stem cells: isolation and characterization of the cells and their osteogenic differentiation potential on embroidered and surface-modified polycaprolactone-co-lactide scaffolds. In Vitro Cell Dev. Biol. Anim. 46, 624-634.

Rozemuller, H., Prins, H.J., Naaijkens, B., Staal, J., Bühring, H.J., Martens, A.C., 2010. Prospective isolation of mesenchymal stem cells from multiple mammalian species using cross- reacting anti-human monoclonal antibodies. Stem Cells Dev. 19, 1911-1921.

Seed, T.M., Husseini, S.G., Knospe, W.H., 1986. Hematopoiesis on cellulose ester membranes: VII. Ultrastructure of stroma of marrow-enriched membranes with trilineal hematopoiesis. Exp. Hematol. 14, 108-118.

Somoza, R.A., Acevedo, C.A., Albornoz, F., Luz-Crawford, P., Carrión, F., Young, M.E., Weinstein-Oppenheimer, C., 2015. TGFβ3 secretion by three-dimensional cultures of human

dental apical papilla mesenchymal stem cells. J. Tissue Eng. Regen. Med. 2015. Feb 18. doi: 10.1002/term.2004.

Takayama, T., Kondo, T., Kobayashi, M., Ohta, K., Ishibashi, Y., Kanemaru, T., Shimazu, H., Ishikawa, F., Nakamura, T., Kinoshita, S., Nakamura, K., 2009. Characteristic morphology and distribution of bone marrow derived cells in the cornea. Anat. Rec.292, 756-763.

Varki, A., Lowe, B., 2009. Biological roles of glycans. In: Varki, A. et al. (Eds) Essentials of Glycobiology, II edition. Cold Spring Harbor Laboratory Press, New York, pp. 75-99.

Wiesmann, A., Bühring, H.J., Mentrup, C., Wiesmann, H.P., 2006. Decreased CD90 expression in human mesenchymal stem cells by applying mechanical stimulation. Head Face Med. 2:8.

Woodbury, D., Schwarz, E.J., Prockop, D.J., Black, I.B., 2000. Adult rat and human bone marrow stromal cells differentiate into neurons. J. Neurosci. Res. 61, 364-370.

Legends

Fig. 1. Morphological characteristics of oBM-MSCs culture. The cells exhibit flattened or fibroblast-like morphology. Scale bar= 260 μm.

Fig. 2. Flow cytometric analysis of oBM-MSCs. The mean fluorescence intensity of cell populations is reported on the x-axis. Black line curves show the fluorescence peaks and gray line curves represent the negative control. The positive cells are gated in M1.

Fig. 3. Light micrograph of oBM-MSCs culture showing the presence of cells different in shape and staining intensity. Toluidine blue staining. Scale bar = 10 μm.

Fig. 4. Electron micrographs showing electron-lucent cells. e, endosome; g, glycogen aggregate; Ga, Golgi apparatus; m, mitochondrium; N, nucleus; rER, rough endoplasmic reticulum; arrow, coated vesicle suggestive of receptor-mediated endocytosis; arrowhead, secretory vesicles; double arrowheads, intercellular junctions. Scale bars: A= 2 μm; B= 0.5 μm; C,D,E,F = 0.1 μm.

Fig. 5. Electron micrographs of electron-lucent cells characterized by vacuoles and secondary lysosomes. B shows high magnification of the square-marked zone from A. m, mitochondrium. Scale bars: A= 2.5 μm; B= 0.5 μm.

Fig. 6. Electron micrographs of type A (A,B,C) and type B (D,E,F) electron-dense cells. g, glycogen aggregate; l, lipid drop; m, mitochondrium; N, nucleus; rER, rough endoplasmic reticulum; arrow, filopodia; double arrows, intercellular junctions; double arrowheads, pseudopodia. Circled area shows cytoplasmic connections between electron-lucent cells and type B electron-dense cells. Scale bars: A= 2 μm; B= 0.2 μm; C,E= 0.3 μm; D= 1 μm; F = 0.5 μm.

Fig. 7. Electron micrographs showing immunogold labelling of CD90 antigen on oBM-MSCs culture surface (arrow). dc, electron-dense cell; lc, electron-lucent cell. Scale bars: A = 0.25 μm; B= 0.30 μm.

Figure 1

Click here to download high resolution image

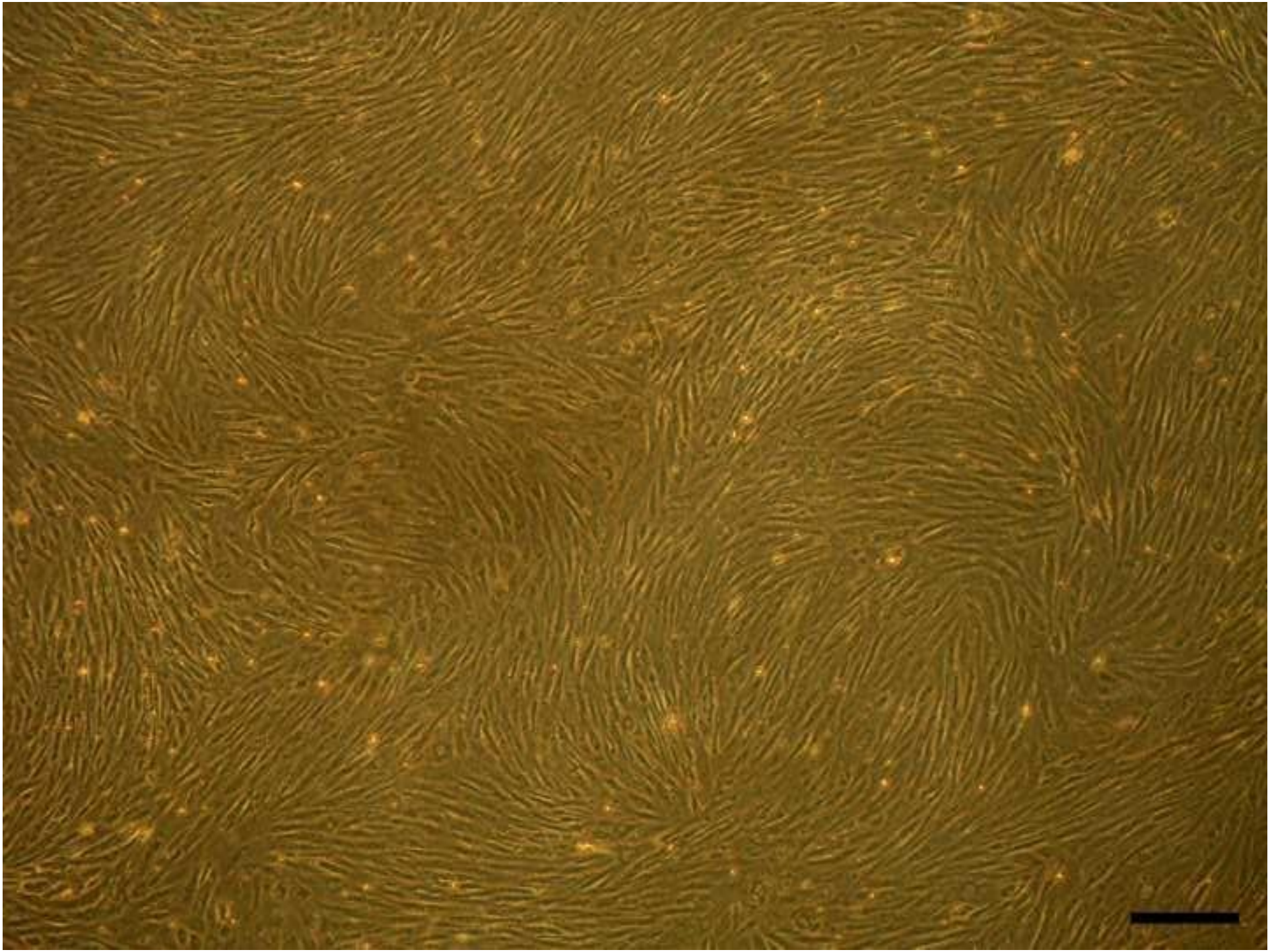

Figure 2

Click here to download high resolution image

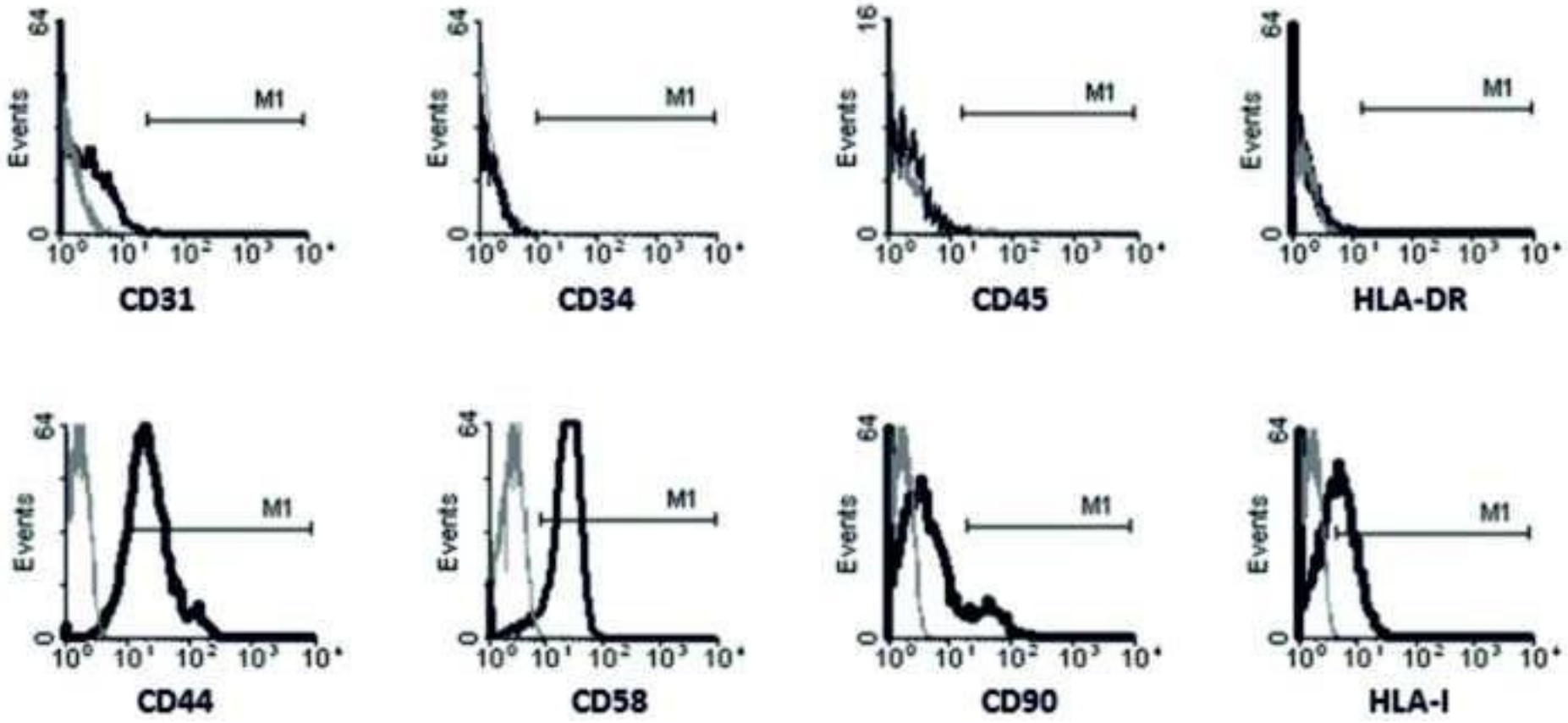

Figure 3

Click here to download high resolution image

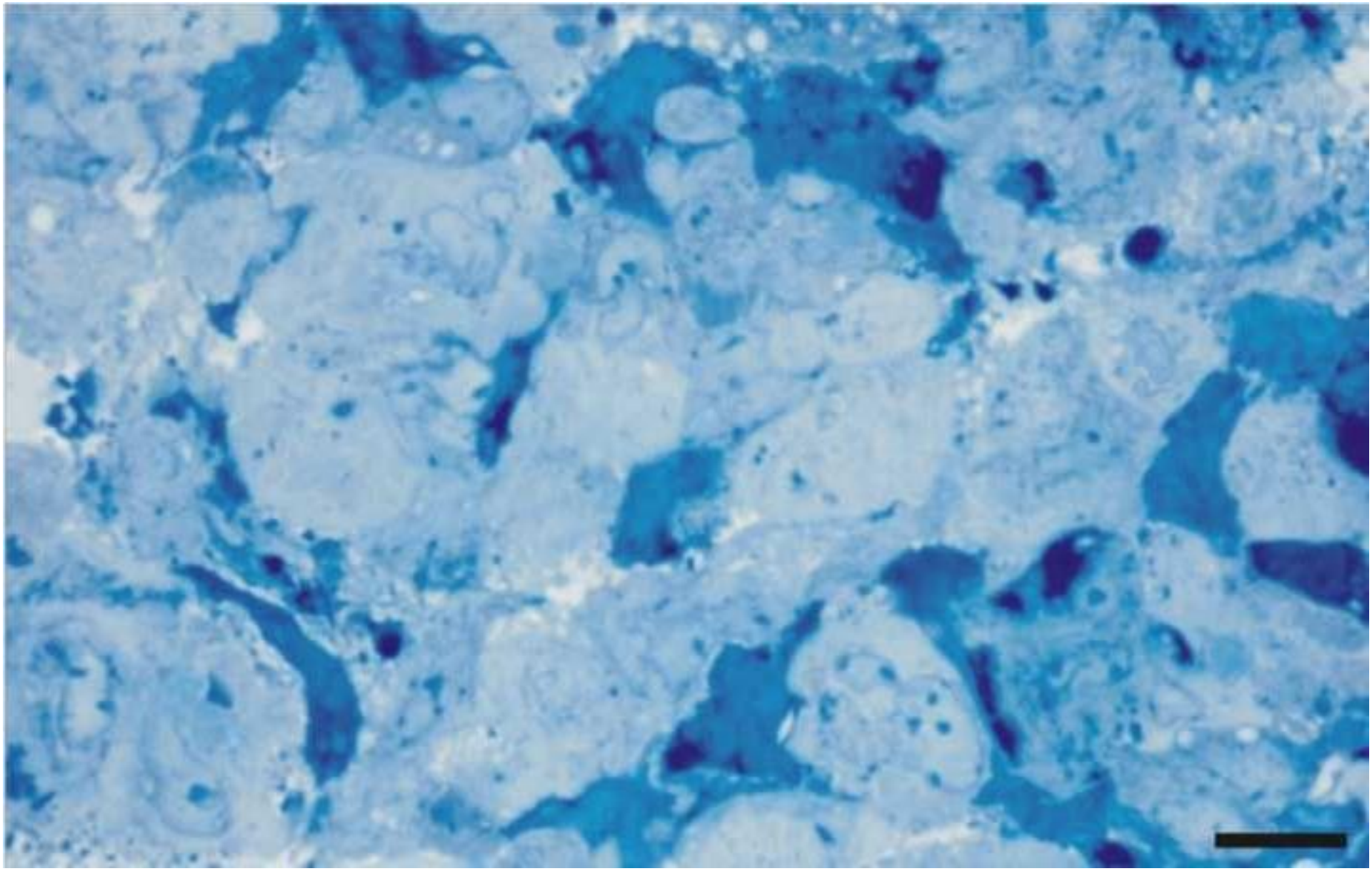

Figure 4

Click here to download high resolution image

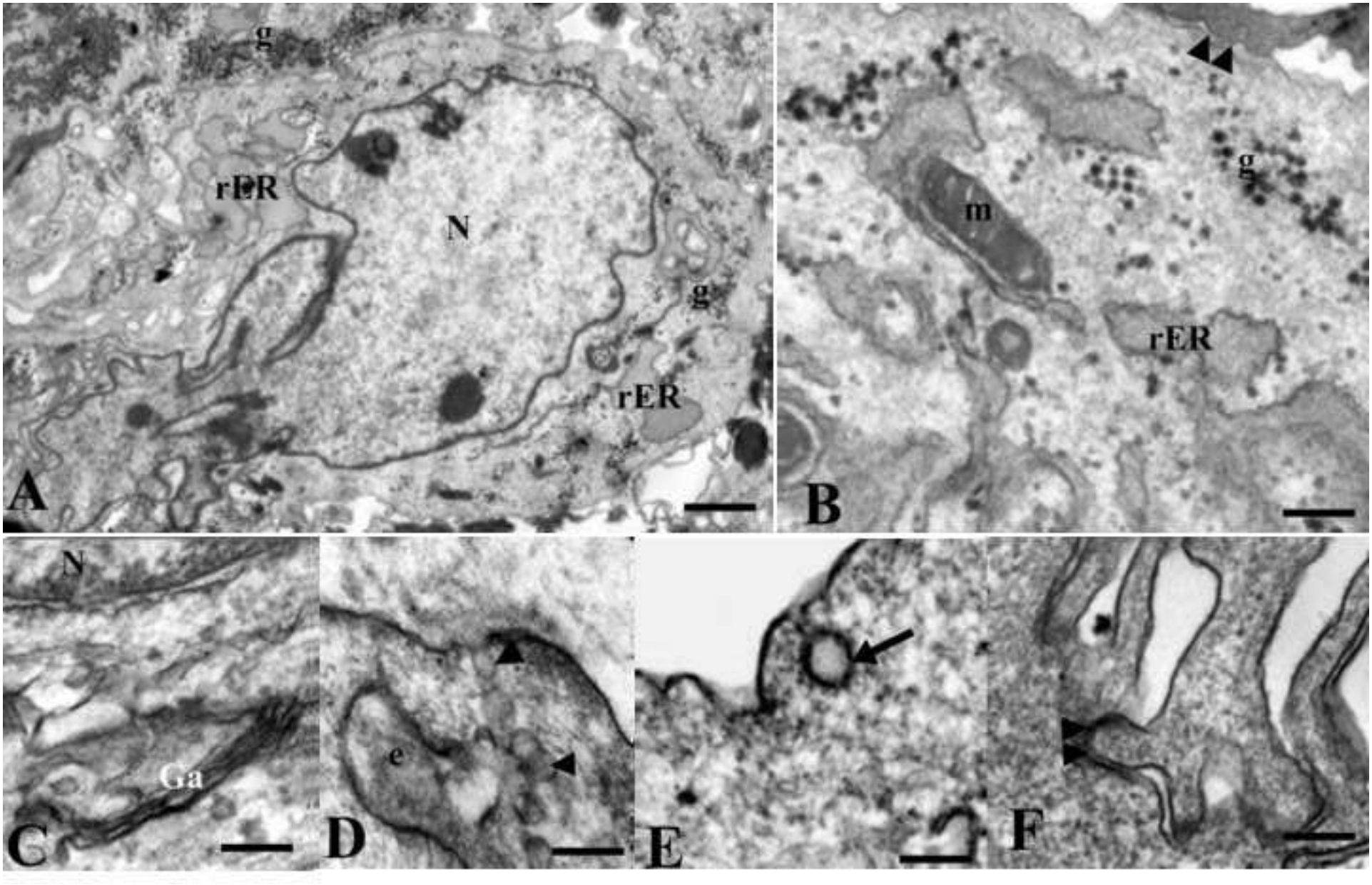

Figure 5

Click here to download high resolution image

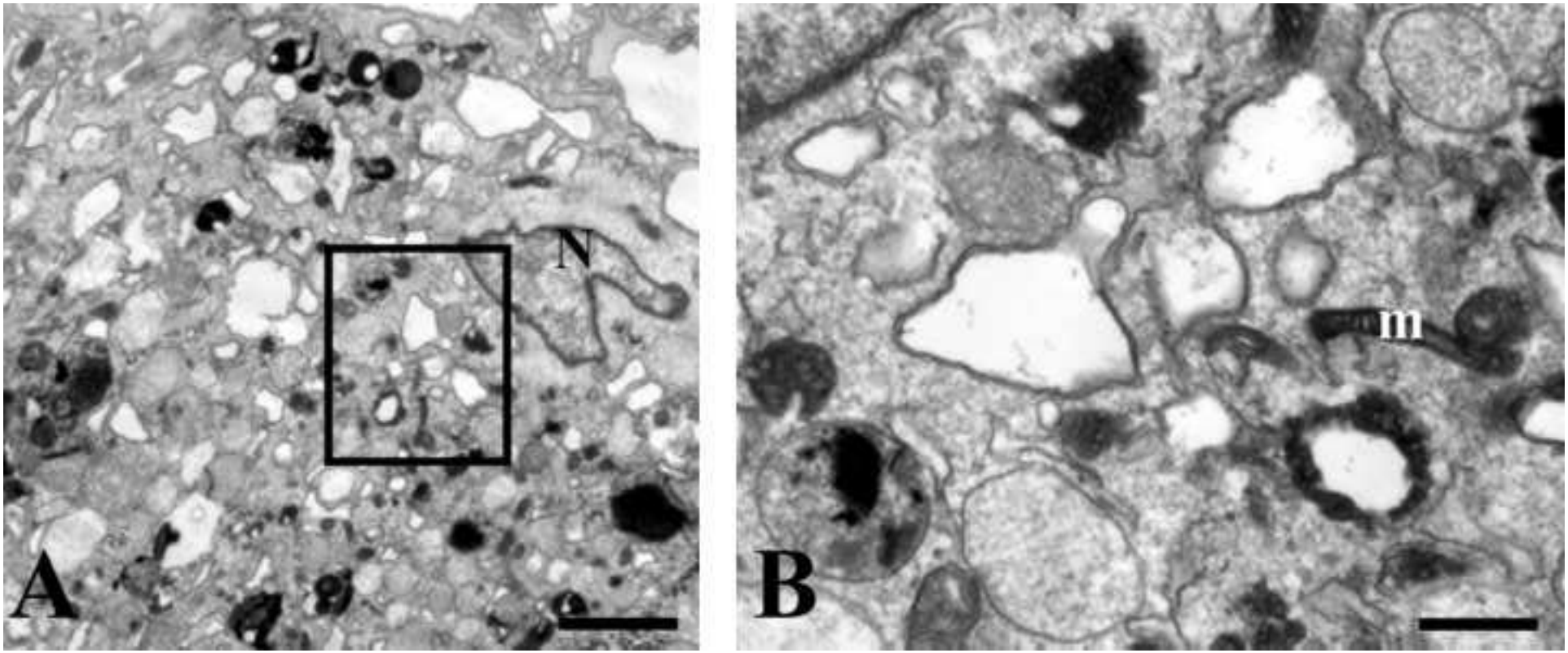

Figure 6

Click here to download high resolution image

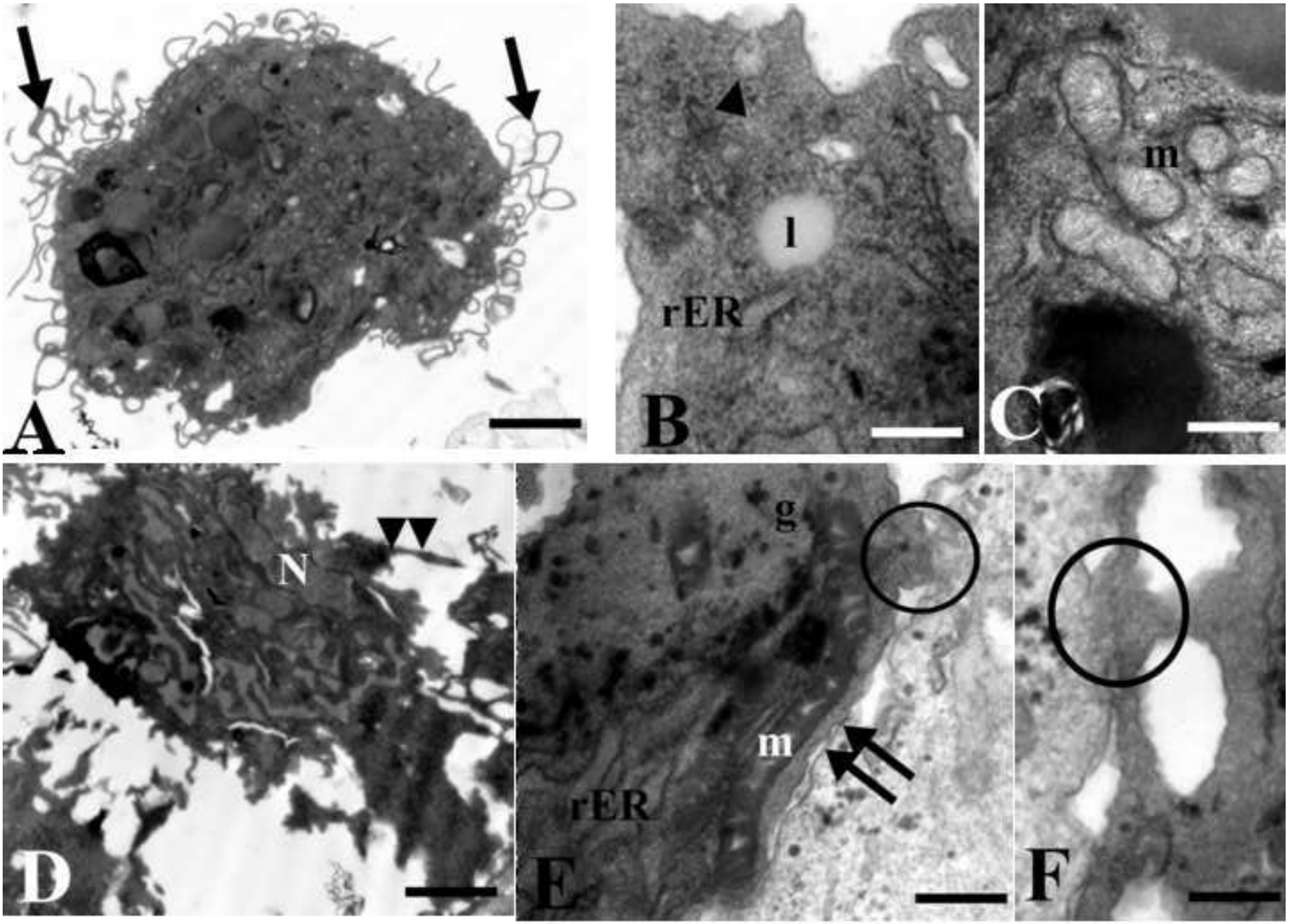

Figure 7

Click here to download high resolution image